

## Light scattering and Fano resonances in high- $Q$ photonic crystal nanocavities

M. Galli,<sup>1,a)</sup> S. L. Portalupi,<sup>1</sup> M. Belotti,<sup>1</sup> L. C. Andreani,<sup>1</sup> L. O'Faolain,<sup>2</sup> and T. F. Krauss<sup>2</sup>

<sup>1</sup>*Dipartimento di Fisica "A. Volta" and UdR CNISM, Università di Pavia, 27100 Pavia, Italy*

<sup>2</sup>*School of Physics and Astronomy, University of St. Andrews, Fife KY16 9SS, United Kingdom*

(Received 5 December 2008; accepted 21 January 2009; published online 17 February 2009)

The authors show that light scattering from high- $Q$  planar photonic crystal nanocavities can display Fano-like resonances corresponding to the excitation of localized cavity modes. By changing the scattering conditions, we are able to tune the observed lineshapes from strongly asymmetric and dispersivelike resonances to symmetric Lorentzians. Results are interpreted according to the Fano model of quantum interference between two coupled scattering channels. Combined measurements and line shape analysis on a series of silicon  $L3$  nanocavities as a function of nearby hole displacement demonstrate that  $Q$  factors as high as  $1.1 \times 10^5$  can be directly measured in these structures. Furthermore, a comparison with theoretically calculated  $Q$  factors allows to extract the rms deviation of hole radii due to weak disorder of the photonic lattice. © 2009 American Institute of Physics. [DOI: 10.1063/1.3080683]

High- $Q$  optical nanocavities are increasingly gaining interest in many diverse areas of research, ranging from nanophotonics<sup>1-3</sup> and biochemical sensing<sup>4</sup> to cavity quantum electrodynamics.<sup>5,6</sup> Their ability to concentrate electromagnetic fields in extremely small spatial regions is a key to strong radiation-matter interaction, which makes them ideal tools for the study and exploitation of physical phenomena at a nanoscale level. Planar photonic crystal (PhC) nanocavities, obtained by two-dimensional patterning of a slab waveguide, are of special interest due to their compactness and ease of fabrication. Ultrahigh- $Q$  factors with mode volumes down to a cubic wavelength have been recently demonstrated in these systems.<sup>3,7</sup>

Optical characterization of high- $Q$  planar PhC nanocavities, i.e., measurement of their resonance frequency and quality factor, is a vital, though nontrivial task. At resonance with a cavity mode, the electromagnetic field is strongly confined in the slab core, being only very weakly coupled to free-space continuum. Current experimental approaches to this problem have mainly focused on either the internal light source method, or on evanescent coupling to an optical waveguide. The first approach, which is applicable to active-material-based nanocavities, may be however limited by optical absorption and/or pump-induced losses of the active medium. While in some cases high  $Q$ s are measured despite the presence of quantum dots,<sup>8,9</sup> in other cases these affect the maximum measurable  $Q$  factor of the nanocavity.<sup>10,11</sup> On the other hand, the second approach is well suited for passive nanocavities, but it requires the fabrication of additional coupling waveguides or fiber tapers, which complicate the experimental geometry and also may induce a "loading" effect on the cavity that can be avoided only by a careful control of coupling conditions.<sup>8,9,12</sup>

Recently, an alternative technique based on crossed-polarized resonant scattering of laser pulses has proved to be very promising for an easy and quick characterization of cavity modes in InP-based planar PhC nanocavities.<sup>13</sup> Here, by using a similar technique, we show that light scattering from

high- $Q$  silicon PhC nanocavities exhibits strongly asymmetric Fano-like resonances, whose lineshape can be tailored by changing the excitation conditions. A detailed lineshape analysis allows us to uncover the basic features of Fano interference for a single optical two-level system. In addition, this approach yields an accurate tool for determining the  $Q$  factor in a passive cavity without introducing any perturbing contribution and with a spectral resolution limited only by the laser linewidth.

Silicon planar PhC nanocavities consisting of three missing holes along the  $\Gamma$ - $K$  direction in a triangular lattice of air-holes ( $L3$ ) were fabricated by means of e-beam lithography and reactive ion etching on a silicon-on-insulator wafer (220 nm thick silicon on 2000 nm of silica purchased from SOITEC). Airbridged PhC nanocavities were then created through wet etching of the silica using a solution of hydrofluoric acid (see Ref. 14 for more details of the fabrication). This process has been shown to produce very high quality PhCs.<sup>15</sup> Several  $L3$  cavities with lattice constant  $a = 420$  nm and hole radius  $r/a = 0.29$  have been fabricated. Optimization of radius and position of the holes adjacent to the cavity has been performed to obtain high- $Q$  factors.<sup>12,16</sup>

Continuous-wave (cw) light scattering from the planar PhC nanocavities was measured using the experimental geometry shown in Fig. 1(a). Light from an external-cavity tunable laser (1 pm resolution) is linearly polarized by the polarizer  $P$  and focused on the sample by means of a high numerical aperture ( $NA = 0.8$ ) polarization-preserving objective lens. The backward scattered light is collected by a beam splitter and analyzed in crossed polarization by means of the analyzer  $A$ . The sample is oriented so that the cavity axis forms an angle of  $45^\circ$  with respect to both the polarizer and the analyzer, as shown in the scanning electron microscope (SEM) image of Fig. 1(b).

For out-of-resonance frequencies the light reflected back by the planar PhC cavity mainly preserves the incoming  $x$ -polarization [see Fig. 1(b)] and it is then filtered out by the  $y$ -polarized analyzer. This provides a small and flat background in the spectra. At resonance with the cavity mode, however, part of the incoming  $x$ -polarized radiation interacts

<sup>a)</sup>Electronic mail: galli@fisicavolta.unipv.it.

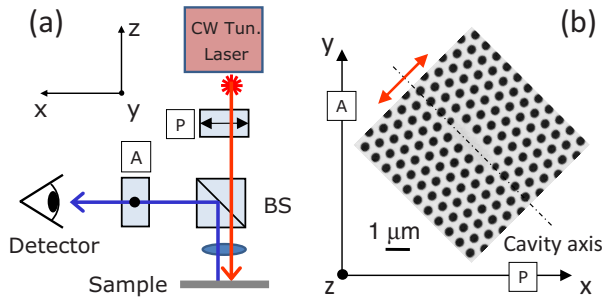


FIG. 1. (Color online) (a) Schematic of the experimental setup for cw light scattering measurements in crossed polarizations. (b) SEM image of an L3 PhC nanocavity, showing its orientation with respect to polarizer and analyzer for obtaining maximum coupling. Red arrow indicates the polarization of the fundamental cavity mode (TE-like).

with the  $xy$ -polarized cavity mode, thus producing a net  $y$ -polarized component in the reflected beam. This passes through the analyzer and is revealed by the detector. This way, even the weak optical response of the cavity mode, which is of the order of one per thousand of incident light power, can be easily detected. Notice that with a cavity axis along  $x$  or  $y$  directions no signal is observed, as expected.

A typical scattering spectrum, obtained by tightly focusing the laser beam (spot diameter  $d_1 \sim 2 \mu\text{m}$ ) onto a PhC nanocavity is shown in Fig. 2(a). A strongly asymmetric peak with a dispersivelike shape is observed as the laser frequency is scanned across the resonance. On the other hand, Fig. 2(b) shows a scattering spectrum of the same PhC nanocavity measured with a slightly defocused laser spot on the sample (spot diameter  $d_2 \sim 10 \mu\text{m}$ ). An almost perfectly symmetric

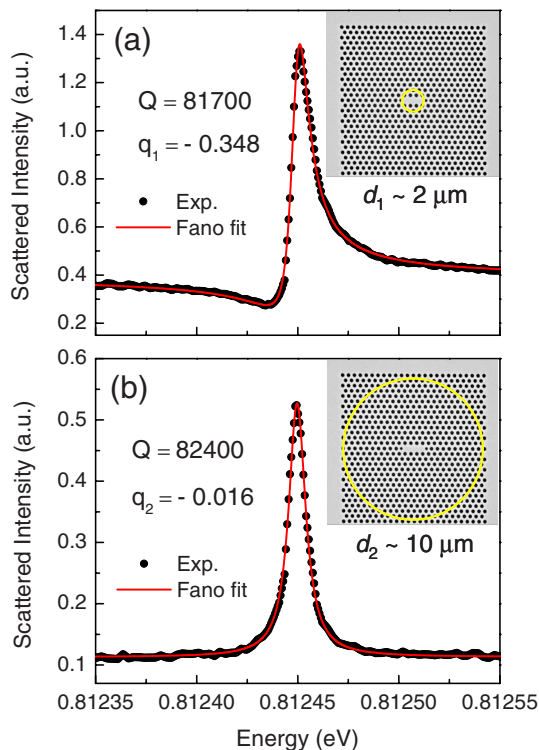


FIG. 2. (Color online) Experimental scattering spectra (dots) and best-fits to the Fano lineshape Eq. (1) (red line) of a L3 PhC nanocavity for two different excitation conditions (a) by tightly focusing the laser beam on the nanocavity and (b) by slightly defocusing it. Spot diameters  $d_1$  and  $d_2$  with respect to the nanocavity dimensions are shown in the insets (yellow circles) for the two cases.

peak is observed in this case. This result can be fully explained in the framework of the Fano quantum interference effect, which describes the configuration interaction between two coupled channels in a scattering problem.<sup>17</sup> The effect arises whenever the scattering from an input state can take place via two distinct pathways, either *directly* toward a continuum of extended states or *resonantly* through a discrete energy level. The interference between these different configurations gives rise to an asymmetric lineshape. Although Fano resonances in light scattering are very popular,<sup>18–21</sup> attention has been paid most often to periodic systems, while here we are dealing with a localized scattering center (the cavity). In our case, the two interfering scattering amplitudes correspond to light that is directly (nonresonantly) reflected by the PhC pattern, which gives rise to the small continuum background signal, and light that is resonantly coupled to the cavity mode and then reflected back toward the continuum.

Without entering the details of the specific scattering dynamics and keeping sight of the underlying physical picture, we can fit the scattering data with the Fano lineshape

$$F(\omega) = A_0 + F_0 \frac{[q + 2(\omega - \omega_0)/\Gamma]^2}{1 + [2(\omega - \omega_0)/\Gamma]^2}, \quad (1)$$

where  $\omega_0$  is the frequency of the cavity mode,  $\Gamma$  is the resonance linewidth, and  $A_0$  and  $F_0$  are constant factors. According to Fano's original work,<sup>17</sup> the dimensionless parameter  $q$  describes the ratio between resonant and nonresonant transition amplitudes in the scattering process. It accounts for the lineshape asymmetry and can assume either positive or negative values. By looking at Eq. (1) the three following distinct regimes can be recognized: (i) for  $|q|$  values of the order of unity, i.e., when resonant and direct scattering amplitudes are comparable with each other, a strongly asymmetric resonance is observed; (ii) when  $|q|$  is large, meaning that resonant scattering dominates over direct scattering, the observed lineshape tends toward a symmetric Lorentzian; (iii) finally, for small  $|q|$  values, i.e., when resonant scattering is small compared to direct (background) scattering, the Fano profile takes the form of a reversed Lorentzian. This said, the best-fitting curves to experimental data measured for tight focus and defocused conditions are shown in Figs. 2(a) and 2(b), respectively. We notice that experimental curves are very well fitted by Eq. (1), which yields the values  $q_1 = -0.348$  and  $q_2 = -0.016$  in the two cases. The observed change in resonant lineshape upon changing the excitation conditions is now clear: an increase in the excitation area with respect to the cavity area leads to a decrease in the resonant scattering amplitude over the nonresonant one. This is demonstrated by both the lowering of the  $q$  parameter and by the observation of an almost symmetric (Lorentzian) lineshape (notice that a negative peak is transformed into a positive one by the use of crossed polarization detection). Indeed, by comparing the ratio of the two different excitation areas ( $s_2/s_1 \sim 25$ ) to the ratio of fitted  $q$  values ( $q_1/q_2 \sim 22$ ) we notice a close correspondence. Thus, by changing the excitation conditions we are able to tune the Fano interference effect in our PhC nanocavity, a feature that is crucially related to the presence of a localized cavity mode.

The best fit of scattering spectra from PhC nanocavities with the Fano lineshape Eq. (1) also yields a precise determination of their resonance energy and quality factor  $Q$ . By comparing the results shown in Figs. 2(a) and 2(b), we ob-

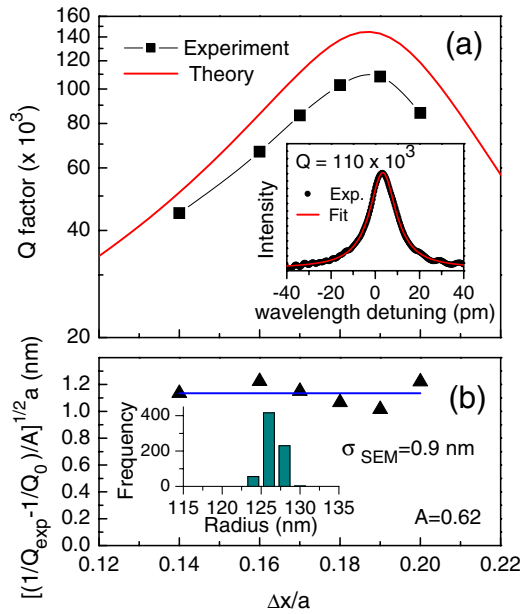


FIG. 3. (Color online) (a) Experimentally determined (dots)  $Q$ -factors compared to calculated ones for a series of  $L3$  PhC nanocavities as a function of the adjacent hole shift  $\Delta x/a$ . The scattering spectrum (dots) and best-fit (red line) for the highest  $Q$  nanocavity is shown in inset. (b) Disorder parameter  $\sigma$  determined from the experimental results. The inset shows the distribution of hole radii determined from SEM analysis.

serve that the measured mode energies and  $Q$  values are almost independent of the excitation conditions. Indeed, the relative difference between the fitted  $Q$  values in the two cases is only 0.85%, which is well within the fit error of 1.1% on the  $Q$  factor. The combined use of resonant scattering and lineshape analysis could then be very useful for accurate characterization of planar PhC nanocavities. To demonstrate this ability, we measured and analyzed the scattering spectra from a series of  $L3$  PhC nanocavities with different optimization parameters. Figure 3(a) shows the evolution of the measured  $Q$  factor as a function of the adjacent hole shift  $\Delta x/a$ . Due to the “gentle” confinement effect,<sup>12</sup> the  $Q$  factor increases up to a maximum value of  $1.1 \times 10^5$  for  $\Delta x/a = 0.19$ . We notice that this is the highest reported  $Q$  factor for a silicon  $L3$  nanocavity, obtained by tuning the nearest neighbor holes only. Measured  $Q$  factors are in good agreement with calculated ones all over the  $\Delta x/a$  range, although maximum theoretical  $Q$  values ( $1.5 \times 10^5$ ) are slightly larger than measured ones. Agreement is better for lower  $Q$  cavities, suggesting that fabrication imperfections and/or surface roughness (that contribute an additive factor to the inverse  $Q$ ) are indeed the limiting factor for  $L3$  nanocavities. To estimate the disorder parameter  $\sigma$  in our system—defined as the root-mean-square deviation of the hole radii—we notice<sup>22</sup> that the radiative loss due to disorder scattering scales as  $\propto \sigma^2$  and consider the relation  $1/Q_{\text{exp}} = 1/Q_0 + A(\sigma/a)^2$ , where  $Q_{\text{exp}}$  is the experimental quality factor and  $Q_0$  is the theoretically calculated intrinsic one (without disorder). The factor  $A$  is determined by a theoretical calculation of disorder-induced losses and it depends on the specific geometry of the nanocavity,<sup>22</sup> taking the value of 0.62 in our case. By inverting this relation, the disorder parameter  $\sigma$  can be evaluated for the different nanocavities, as shown in Fig.

3(b). All of the nanocavities display almost the same value  $\sigma \sim 1.1$  nm, which compares very well with  $\sigma_{\text{SEM}} \sim 0.9$  nm, as determined by SEM image analysis [Fig. 3(b) inset]. A slightly higher value of  $\sigma$  is indeed expected from optical measurements, as they probe all disorder contributions beyond the hole size variations visible from SEM.

In conclusion, we have shown that light scattering by  $L3$ -type silicon planar PhC nanocavities gives rise to Fano-like resonances with  $Q$ -factors as high as  $1.1 \times 10^5$ . A detailed lineshape analysis for different excitation conditions allows us to tailor the Fano quantum interference effect for a localized optical scattering center. The disorder parameter of the photonic lattice is also determined by comparison with theory. The resonant scattering approach yields an accurate and loadless characterization of high- $Q$  nanocavities, which may be important in view of their manifold applications.

This work was supported by MIUR through FIRB project “Miniaturized electronic and photonic systems” and by Fondazione Cariplo. The fabrication was carried out in the framework of the ePIXnet Nanostructuring Platform for Photonic Integration (see <http://www.nanophotonics.eu>).

- <sup>1</sup>D. K. Armani, T. J. Kippenberg, S. M. Spillane, and K. J. Vahala, *Nature (London)* **421**, 925 (2003).
- <sup>2</sup>T. Tanabe, M. Notomi, E. Kuramochi, A. Shinya, and H. Taniyama, *Nat. Photonics* **1**, 49 (2007).
- <sup>3</sup>S. Noda, M. Fujita, and T. Asano, *Nat. Photonics* **1**, 449 (2007).
- <sup>4</sup>F. De Angelis, M. Patrini, G. Das, I. Maksymov, M. Galli, L. Businaro, L. C. Andreani, and E. Di Fabrizio, *Nano Lett.* **8**, 2321 (2008).
- <sup>5</sup>T. Aoki, B. Dayan, E. Wilcut, W. P. Bowen, A. S. Parkins, T. J. Kippenberg, K. J. Vahala, and H. J. Kimble, *Nature (London)* **443**, 671 (2006).
- <sup>6</sup>K. Hennessy, A. Badolato, M. Winger, D. Gerace, M. Atatüre, S. Gulde, S. Fält, E. L. Hu, and A. Imamoglu, *Nature (London)* **445**, 896 (2007).
- <sup>7</sup>B. S. Song, S. Noda, T. Asano, and Y. Akahane, *Nature Mater.* **4**, 207 (2005).
- <sup>8</sup>K. Srinivasan and O. Painter, *Appl. Phys. Lett.* **90**, 031114 (2007).
- <sup>9</sup>K. Srinivasan, A. Stintz, S. Krishna, and O. Painter, *Phys. Rev. B* **72**, 205318 (2005).
- <sup>10</sup>J. Hendrickson, B. C. Richards, J. Sweet, S. Mosor, C. Christenson, D. Lam, G. Khitrova, H. M. Gibbs, T. Yoshie, A. Sherer, O. B. Shchekin, and D. G. Deppe, *Phys. Rev. B* **72**, 193303 (2005).
- <sup>11</sup>M. El Kurdi, X. Checoury, S. David, T. P. Ngo, N. Zerounian, P. Boucaud, O. Kermarrec, Y. Campidelli, and D. Bensahel, *Opt. Express* **16**, 8780 (2008).
- <sup>12</sup>Y. Akahane, T. Asano, B. S. Song, and S. Noda, *Nature (London)* **425**, 944 (2003).
- <sup>13</sup>M. McCutcheon, G. W. Rieger, I. W. Cheung, J. F. Young, D. Dalacu, S. Frédéric, P. J. Poole, G. C. Aers, and R. Williams, *Appl. Phys. Lett.* **87**, 221110 (2005).
- <sup>14</sup>J. Li, T. P. White, L. O’Faolain, A. Gomez-Iglesias, and T. F. Krauss, *Opt. Express* **16**, 6227 (2008).
- <sup>15</sup>L. O’Faolain, X. Yuan, D. McIntyre, S. Thoms, R. M. De La Rue, and T. F. Krauss, *Electron. Lett.* **42**, 1454 (2006).
- <sup>16</sup>L. C. Andreani, D. Gerace, and M. Agio, *Photonics Nanostr. Fundam. Appl.* **2**, 103 (2004).
- <sup>17</sup>U. Fano, *Phys. Rev.* **124**, 1866 (1961).
- <sup>18</sup>V. N. Astratov, D. M. Whittaker, I. S. Culshaw, R. M. Stevenson, M. S. Skolnick, T. F. Krauss, and R. M. De La Rue, *Phys. Rev. B* **60**, R16255 (1999).
- <sup>19</sup>S. Fan and J. D. Joannopolulos, *Phys. Rev. B* **65**, 235112 (2002).
- <sup>20</sup>T. W. Ebbesen, H. J. Lezec, H. F. Ghaemi, T. Thio, and P. A. Wolff, *Nature (London)* **391**, 667 (1998).
- <sup>21</sup>X. Yang, C. Husko, C. W. Wong, M. Yu, and D. L. Kwong, *Appl. Phys. Lett.* **91**, 051113 (2007).
- <sup>22</sup>D. Gerace and L. C. Andreani, *Photonics Nanostruct. Fundam. Appl.* **3**, 120 (2005).